Nuclear Inst. and Methods in Physics Research, A 927 (2019) 301–305

Contents lists available at ScienceDirect

Nuclear Inst. and Methods in Physics Research, A

journal homepage: www.elsevier.com/locate/nima

Development of a SiPM-based CsI(Tl) spectrometer with gain stabilization designs for rapid temperature variations

Pin Gong [a,b], Zhenyang Han [a], Le Gao [a], Peng Wang [a], Jinzhao Zhang [c], Xiaobin Tang [a,b,*]

[a] Department of Nuclear Science and Engineering, Nanjing University of Aeronautics and Astronautics, Nanjing 210016, China
[b] Jiangsu Key Laboratory of Nuclear Energy Equipment Materials Engineering, Nanjing 210016, China
[c] National Ocean Technology Center, Tianjin 300112, China

ARTICLE INFO

Keywords:
Silicon photomultiplier
Gain stabilization
FPGA
Temperature correction

ABSTRACT

A spectrometer employing a silicon photomultiplier (SiPM) based scintillation detector has spectrum drift issues under temperature variations. Although some temperature-dependent compensation methods are reported, spectrum distortions under rapid temperature fluctuations have received little attention. We have developed a SiPM-based CsI(Tl) spectrometer and proposed gain stabilization designs to settle this problem. A temperature sensor was coupled to the SiPM in the detector and wrapped with a thermal insulation foam material to acquire the temperature of the SiPM. Meanwhile, a temperature correction module was applied in the field-programmable gate array (FPGA) within a custom multichannel analyzer (MCA). The effectiveness of the temperature correction module in the FPGA and a specialized detector design were studied and verified under slow and rapid temperature variations. The results prove that the spectrum drifts of the SiPM-based CsI(Tl) spectrometer under rapid temperature variations can be significantly constrained with the proposed gain stabilization designs.

1. Introduction

A silicon photomultiplier (SiPM) is a kind of avalanche photodiodes array operated at Geiger mode, also known as multi-pixel photon counter (MPPC) with excellent features including high gain, insensitivity to magnetic fields, low bias voltage and compact size [1–3]. The SiPM has been widely used in different applications such as nuclear safety, medical imaging and high-energy physics experiments [4–7], however, the SiPM gain is sensitive to temperature [8]. Temperature variations may lead to gain instability of the SiPM-based systems. Passive gain stabilization methods can be realized by keeping the SiPM temperature under control, similar to the temperature control technology used for semiconductor detectors [9]. Active gain stabilization methods by adjusting the bias voltage [10–13] or the gain of the amplifier [14,15] according to the temperature of the SiPM have been reported. However, the effect of the rate of temperature change on the performance of the temperature-dependent gain stabilization method has not been given enough attention. Predictably, because of the temporal temperature differences between the SiPM-based detector and temperature sensor [14], the gain compensation results by these methods may diverge from the actual values when the detector encounters rapid temperature variations.

We have recently developed a digital spectrometer employing a compact SiPM-based CsI (Tl) scintillation detector for the use of γ radiation monitoring and radionuclide identification applications [16]. In order to solve the problems mentioned above, a temperature sensor was thermally coupled to the SiPM and wrapped with a thermal insulation foam material. Then a gain stabilization method was realized by compensating each pulse amplitude from the detector in the field-programmable gate array (FPGA) according to the SiPM temperature. This method needs no extra hardware compared with other gain stabilization methods which use digital-to-analog converters or adjustable high-voltage driver circuits.

2. Materials and methods

2.1. Detector design

The radiation detector is shown in Fig. 1. A $6 \times 6 \times 10$ mm^3 CsI(Tl) crystal and a Hamamatsu SiPM S13360-6075CS [17] were employed. The SiPM sensitivity is well matched with the CsI(Tl) luminescence spectrum [18]. The CsI(Tl) crystal was coupled to the SiPM by optical grease, and they were wrapped in an aluminum foil to keep out ambient light. The gain instability of the SiPM-based CsI(Tl) scintillation detector is mainly caused by the temperature change of the SiPM. To measure the SiPM temperature, a temperature sensor DS18B20 [19] was coupled to the back of the SiPM by thermal grease. Then, an

* Corresponding author at: Department of Nuclear Science and Engineering, Nanjing University of Aeronautics and Astronautics, Nanjing 210016, China.
E-mail address: tangxiaobin@nuaa.edu.cn (X. Tang).

https://doi.org/10.1016/j.nima.2019.02.058
Received 5 May 2018; Received in revised form 27 January 2019; Accepted 20 February 2019
Available online 22 February 2019
0168-9002/

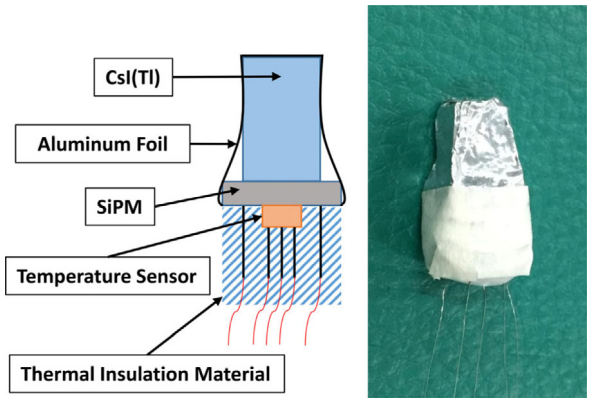

Fig. 1. The structure of the SiPM-based CsI(Tl) detector.

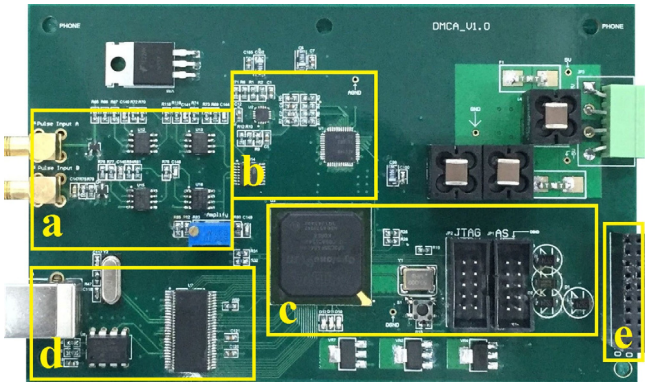

Fig. 2. Photograph of the DMCA board: (a) Analog processing; (b) ADC; (c) FPGA; (d) USB; (e) General-purpose input/output interface.

ethylene-vinyl acetate copolymer (EVA) foam material was used to wrap the SiPM and the temperature sensor together. The EVA foam material is an ideal packaging material which has many advantages, such as heat-insulating, water proof, chemical resistant, collision resistant, and recyclable. Benefiting from the thermal insulation property of the EVA foam, the temperatures of the SiPM and the temperature sensor can arrive in the same time as the ambient temperature changes. The output signals from the temperature sensor and the SiPM were both drawn from the insulation layer using thinner wires to minimum heat conduction.

2.2. DMCA design for gain stabilization

A digital multichannel analyzer (DMCA) board (Fig. 2) has been successfully developed to process the detector's signals and implement gain stabilization. An FPGA chip of Altera Cyclone III series was used with a working frequency of 100 MHz. The signals from the detector were first processed by an analog circuit including an amplifier and a Sallen–Key (S–K) filter, then sampled by an analog to digital converter (ADC) with a sampling rate of 100 MHz. The low voltage differential signaling (LVDS) outputs from the ADC were sent to the FPGA for digital pulse processing. In order to acquire the temperature data of the SiPM in real time, a general-purpose input/output interface (GPIO) was applied for communications between the FPGA and the temperature sensor. A third-generation telecommunication technology used in our previous design portable dose rate detector was also expected to be applied in the DMCA board [20].

The procedure of the digital process in the FPGA is shown in Fig. 3. First, the digital pulses from the ADC were received by the pulse height analyzer (PHA) module to be shaped using a trapezoidal shaper. The

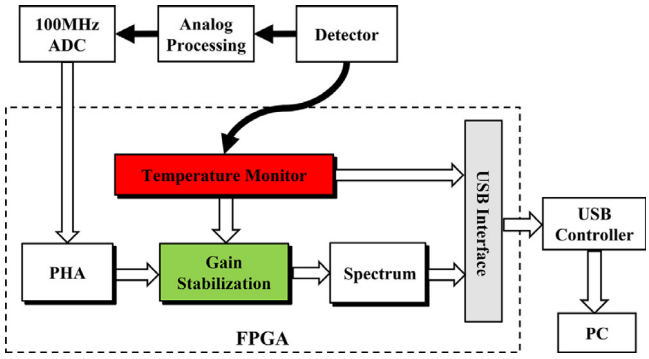

Fig. 3. Diagram of the digital process in the FPGA.

amplitudes of the trapezoidal pulses were acquired after the baseline restoration and the pulse pile-up rejection processes. Simultaneously, the temperature monitor module read the latest temperature of the temperature sensor at each pulse event. A gain stabilization module was invented to correct every pulse amplitude from the PHA module according to the temperature sensor data and a gain correction algorithm. The corrected pulse amplitudes were finally converted into spectra in the FPGA and sent to a computer for spectral analysis.

2.3. Principle of the gain correction method

For a certain γ energy, the variations of the SiPM gains can be reflected by those of the pulse amplitudes from the PHA module linearly, and lead to the shifts of the peak channel. A gain correction factor F is here defined as:

$$F = \frac{G}{G_0} = \frac{A}{A_0} = \frac{C}{C_0} \tag{1}$$

where G is the SiPM gain, G_0 is a reference gain, A is the pulse amplitude at G, A_0 is the pulse amplitude at G_0, C is the peak channel at G, and C_0 is the peak channel at G_0.

Meanwhile, the SiPM gain G is a linear function of the SiPM temperature when the bias voltage is fixed [21], which results in a linear relationship between the gain correction factor F and the SiPM temperature T. That is:

$$F(T) = a + bT \tag{2}$$

The a and b in formula (2) can be obtained by measuring the relative peak positions (C/C_0) at different SiPM temperatures, and thereafter we have:

$$A_0 = \frac{A}{F(T)} = \frac{A}{a + bT} \tag{3}$$

An algorithm based on Formula (3) was programmed in the gain stabilization module in the FPGA. Then every pulse amplitude A from the PHA module corresponding to any SiPM temperature T can be corrected to the reference pulse amplitude A_0, which corresponds to an established reference temperature. So far, the SiPM gain instability under temperature variations is corrected.

2.4. Experimental setup

When applied to environmental radiation monitoring, the SiPM-based detector will encounter temperature fluctuations which could be dramatic sometime. Taking into account of that, this study considered not only slow but also fast temperature changes. A thermal chamber Drick DRK641 was used to study the peak shift in the spectra and to verify the gain stabilization performance under different conditions of temperature variation. The detector and the readout circuits were placed together in the thermal chamber. The spectra measurements

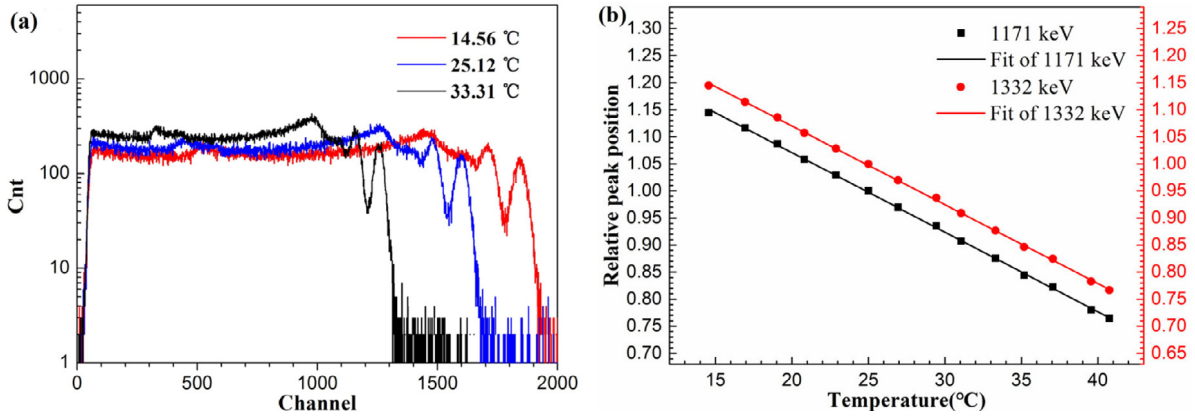

Fig. 4. Peak shifts of the ^{60}Co spectra at different temperatures.

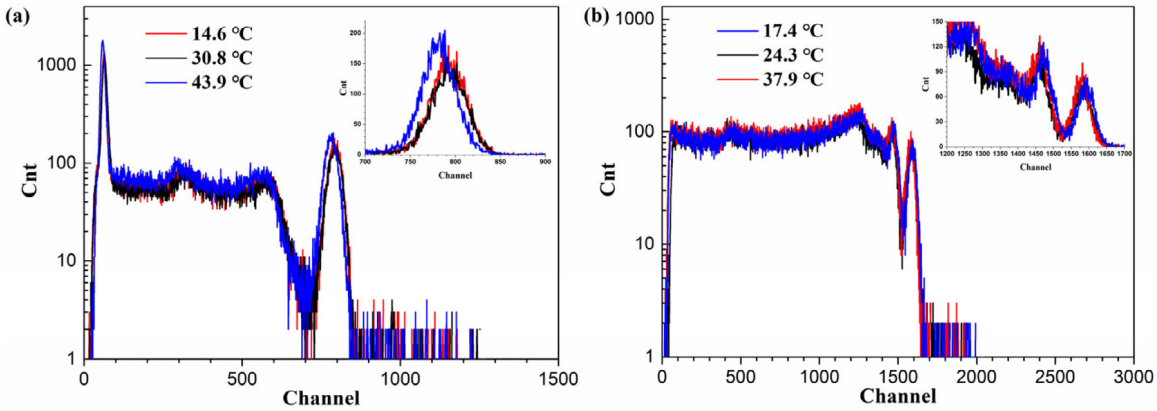

Fig. 5. Stabilized spectra of ^{137}Cs (a) and ^{60}Co (b) measured during different temperature variation periods.

used a 5.29×10^4 Bq ^{137}Cs or a 5.29×10^4 Bq ^{60}Co radioactive source next to the detector. The bias voltage of the SiPM was 56.6 V which was supplied from outside of the thermal chamber. The signals from the detector and the temperature sensor were transferred outside the thermal chamber and input to the DMCA board.

3. Results and discussions

3.1. Determination of the gain correction factor

In order to establish the gain correction factor *F*, we measured the relative peak positions (C/C0) of the ^{60}Co spectra at different SiPM temperatures. The spectra were measured at 14 different temperatures between 15 °C and 40 °C. The light yield of the CsI(Tl) scintillator adopted is almost stable, 55,300 +/− 630 photons/MeV in the range of 15 °C to 40 °C, according to the production information. Every given temperature was kept constant for 3 min before a spectrum measurement. Fig. 4(a) shows the peak shifts at three of these different temperatures. The temperatures were read out by the temperature sensor. The reference temperature was set to 25 °C, and the relative peak positions of 1173 keV and 1332 keV are shown in Fig. 4(b). The relative peak shift from 15 °C to 40 °C is 38%, indicating a gain deviation of −1.46% per degree Celsius. Linear fits were performed for both 1173 keV and 1332 keV, which get same results of parameters *a* and *b* in formula (2). Therefore, the gain correction factor *F* function in Fig. 4 was established and programmed in the gain stabilization module of the FPGA for pulse amplitudes corrections.

3.2. Gain stabilization performances of the spectrometer under relative slow temperature changes

The gain stabilization performance of the spectrometer was tested by measuring ^{60}Co and ^{137}Cs spectra and evaluating their peak positions and energy resolution. The temperature variation rates in the experiments were relatively slow. As shown in Fig. 6, the temperature increased from 10 °C to 45 °C and dropped back to 10 °C twice with the average temperature variation rates of ±1.17 °C/min and ±0.51 °C/min, correspondingly. Fig. 5 shows part of the stabilized ^{137}Cs and ^{60}Co spectra in different temperature variation processes. The measuring time of each spectrum was 5 min. The spectra measured at different temperatures were almost identical, and very small peak shifts were found after the gain stabilization method was carried out. The gain stabilization performance can also be reflected by the shape consistency of each measured energy spectrum.

The peak positions at 662, 1173 and 1332 keV were normalized by the peak position at 25 °C to obtain the relative peak position. As shown in Fig. 6, the experimental results show that the maximum relative peak shift was no more than 3.4% with the gain stabilization module applied, while it was approximately 53.6% without corrections.

The SiPM gain is constantly changing during the temperature changes, indicating that if no stabilization method is used, the peaks will shift continuously and the energy resolution will be decreased. In order to study the improvement of the energy resolution by our method, several spectra without the gain stabilization were also measured. The spectra were fitted and the FWHM was extracted for energy resolution calculations. As shown in Fig. 7, the average energy resolution at 662 and 1332 keV measured before the gain stabilization was 6.3% and 4.4%, respectively. They were improved to 5.8% and 3.7% after the

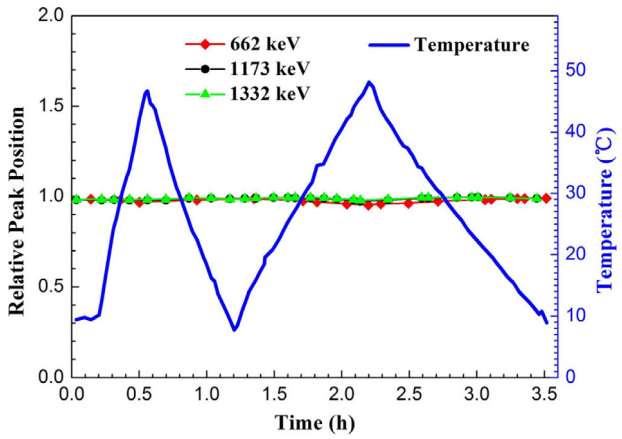

Fig. 6. Relative peak shifts of the spectrometer with the gain stabilization.

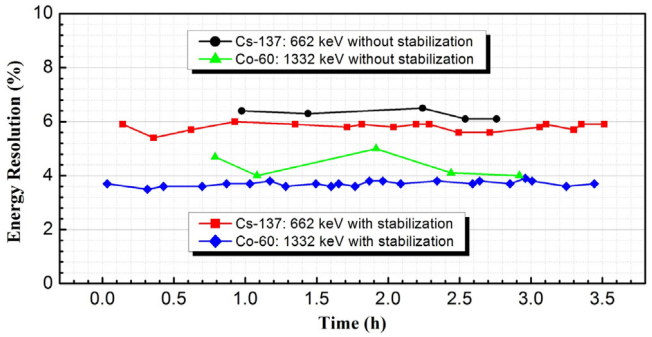

Fig. 7. Energy resolution at 662 and 1332 keV with and without the gain stabilization.

gain stabilization module was applied. These values were close to the energy resolutions measured under constant temperature conditions.

3.3. Gain stabilization performances of the spectrometer under fast temperature changes

3.3.1. Without the thermal insulation layer

The gain stabilization performances of the spectrometer under relative slow temperature changes seems fairly good in the aspect of whether peak shifts or energy resolutions when the gain stabilization module was applied. However, some energy resolution deteriorations were found when temperature changed much faster than that in Section 3.2. It was possibly related to the temperature measurement error caused by the fast temperature variation. To find the cause of the energy resolution deteriorations, an experiment using the designed gain stabilization module without thermal insulation layer was first carried out. To simulate fast temperature variations, the detector was first placed outside of the thermal chamber at an ambient temperature of 14 °C. Then the detector was rapidly transferred into the thermal chamber which was preheated to 40 °C. The energy resolutions were being measured during this process. As shown in Fig. 8(a), the temperatures of the SiPM varied from 14.0 °C to 40.1 °C within 2 min with an average rising rate of 0.20 °C/s. Fig. 8(b) shows the spectra before, in the middle of, and after the fast temperature rising process, and the energy resolutions were 3.7%, 7.2% and 3.7% at 1332 keV, correspondingly. A Gaussian fit was used to extract the peak of the spectrum. The peak of the spectrum in the middle of the fast temperature rising process shifted left compared to those of the spectra under constant temperatures. Based on the results, the correction factor of the spectrum during fast temperature variations was bigger, which means that the temperature of the temperature sensor was greater than that of the SiPM during rapid temperature changes.

3.3.2. With the thermal insulation layer

Although the temperature sensor is thermally coupled to the SiPM, there is always a temperature gradient between them when the external temperature suddenly changes. In addition, the temperature of the temperature sensor rises faster than the SiPM's. Therefore, reducing the temperature differences between the temperature sensor and the SiPM is necessary for a better spectrum stabilization performance. As shown in Fig. 9(a), after the foam thermal insulation layer was attached to the detector, the average temperature rising rate of the temperature sensor was reduced to 0.12 °C/s. The energy resolution at 1332 keV slightly worsened to 4.1% when fast temperature variation occurred compared to the value of 3.8% measured at constant temperature. However, the energy resolution was greatly improved compared with the value of 7.2% measured without the thermal insulation layer (Fig. 8(a)). Fig. 9(b) shows a ^{60}Co spectra measured during different temperature variation periods. The application of the thermal insulation layer for the SiPM-based CsI(Tl) detector effectively improved the spectrum stability during the period of fast temperature variations, also indicating that the temperature differences between the temperature sensor and the SiPM can be reduced by this method.

The energy resolution results in Fig. 9(a) show that some temperature differences still existed after the thermal insulation layer was used for the detector. First, the heat transfer from the environment to the temperature sensor cannot be completely eliminated by the thermal insulation layer, so the temperature of the temperature sensor cannot completely follow that of the SiPM. Second, the temperature differences may exist between the two surfaces of the SiPM when the ambient temperature varies rapidly. The temperature of the surface coupled with the CsI(Tl) scintillator may change slower than that of the surface connected with the temperature sensor.

4. Conclusions

In order to solve the gain instability problem of the SiPM based scintillation detector used during rapid temperature variations, we invented a gain stabilization method. A FPGA-based MCA was developed and a gain correction algorithm was realized. The maximum relative peak shift was reduced from 53.6% to 3.4% after the gain correction was applied when the ambient temperature changed at the rate of ±1.17 °C/min and ±0.51 °C/min between 10 °C and 45 °C. A temperature sensor was thermally coupled to the SiPM and wrapped with a thermal insulation foam material. The energy resolution with the foam thermal insulation layer was greatly improved to 4.1% compared with the value of 7.2% measured without the thermal insulation layer under fast temperature variation conditions. A thermal insulation layer can effectively reduce the temperature differences between the temperature sensor and the SiPM, and improve the energy resolution of the SiPM based spectrometer.

Acknowledgments

Pin Gong and Zhenyang Han contributed equally to this work. This work was supported by the National Natural Science Foundation of China (Grant No. 11675078), the Primary Research and Development Plan of Jiangsu Province (Grant No. BE2017729), the Fundamental Research Funds for the Central Universities (Grant No. NJ20160034), the Project supported by the Postgraduate Research & Practice Innovation Program of Jiangsu Province (Grant No. KYLX16_0353) and the Fundamental Research Funds for the Central Universities, and Project supported by the Foundation of Graduate Innovation Center in NUAA (Grant No. kfjj20170613) and the Fundamental Research Funds for the Central Universities.

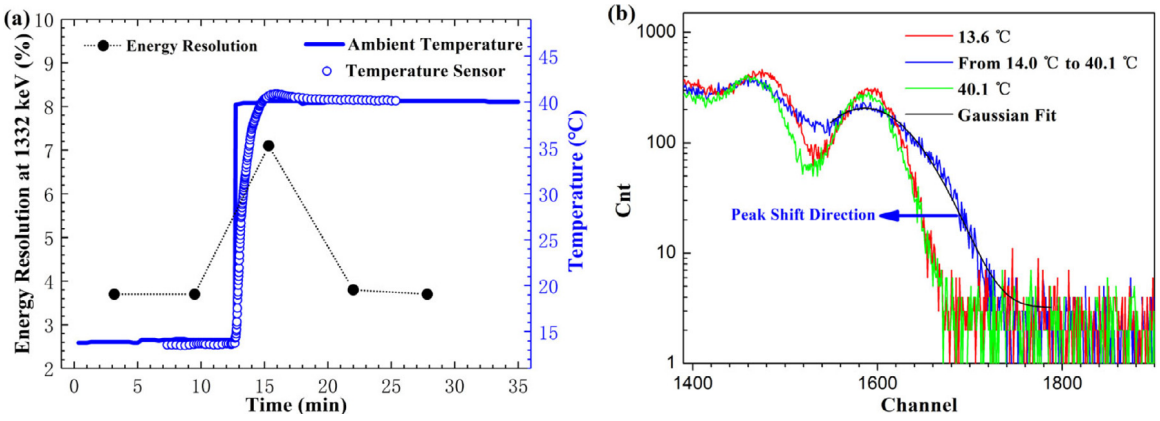

Fig. 8. (a) Energy resolution at 1332 keV and (b) ^{60}Co spectra measured under different temperature conditions without the thermal insulation layer.

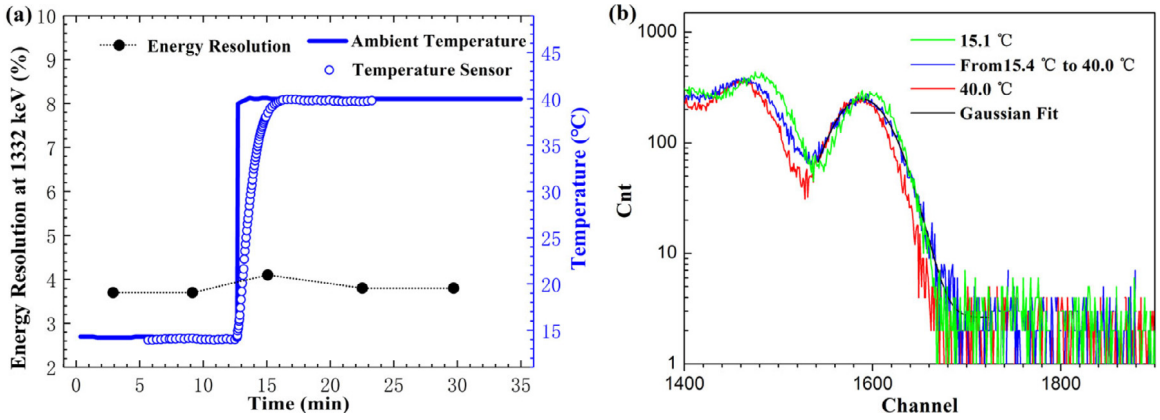

Fig. 9. (a) Energy resolution at 1332 keV and (b) ^{60}Co spectra measured under different temperature conditions using the thermal insulation layer.

References

[1] P. Buzhan, B. Dolgoshein, L. Filatov, et al., Silicon photomultiplier and its possible applications, Nucl. Instrum. Methods Phys. Res. A 504 (2003) 48–52.

[2] V. Saveliev, The recent development and study of silicon photomultiplier, Nucl. Instrum. Methods Phys. Res. A 535 (2004) 528–532.

[3] B. Dolgoshein, V. Balagura, P. Buzhan, et al., Status report on silicon photomultiplier development and its applications, Nucl. Instrum. Methods Phys. Res. A 563 (2006) 368–376.

[4] H.M. Park, K.S. Joo, Performance characteristics of a silicon photomultiplier based compact radiation detector for Homeland Security applications, Nucl. Instrum. Methods Phys. Res. A 781 (2015) 1–5.

[5] D.R. Schaart, H.T.V. Dam, S. Seifert, et al., A novel, SiPM-array-based, monolithic scintillation detector for PET, Phys. Med. Biol. 54 (2009) 3501.

[6] D.J. Herbert, S. Moehrs, N. D'ascenzo, et al., The silicon photomultiplier for application to high-resolution positron emission tomography, Nucl. Instrum. Methods Phys. Res. A 573 (2007) 84–87.

[7] D. Renker, New developments on photosensors for particle physics, Nucl. Instrum. Methods Phys. Res. A 598 (2009) 207–212.

[8] D. Renker, Geiger-mode avalanche photodiodes, history, properties and problems, Nucl. Instrum. Methods Phys. Res. A 567 (2006) 48–56.

[9] K.K. Mahant, A.V. Patel, A. Vala, et al., FPGA based temperature control and monitoring system for X-ray measurement instrument, in: Region 10 Conference, TENCON, 2016 IEEE, 2016, pp. 3249–3252.

[10] P.S. Marrocchesi, M.G. Bagliesi, K. Batkov, et al., Active control of the gain of a 3 mm × 3 mm silicon photomultiplier, Nucl. Instrum. Methods Phys. Res. A 602 (2009) 391–395.

[11] M.Y. Kim, C. Avanzini, M.G. Bagliesi, et al., Scintillation and Cherenkov light detection with a 3 mm × 3 mm silicon photomultiplier, Nuclear Phys. B Proc. Suppl. 197 (2009) 325–330.

[12] P. Dorosz, M. Baszczyk, S. Glab, et al., Silicon photomultiplier's gain stabilization by bias correction for compensation of the temperature fluctuations, Nucl. Instrum. Methods Phys. Res. A 718 (2013) 202–204.

[13] R.A. Shukla, V.G. Achanta, S.R. Dugad, et al., Multi-channel programmable power supply with temperature compensation for silicon sensors, Rev. Sci. Instrum. 87 (2016) 015114.

[14] S. Yamamoto, J. Satomi, T. Watabe, et al., A temperature-dependent gain control system for improving the stability of Si-PM-based PET systems, Phys. Med. Biol. 56 (2011) 2873.

[15] Y. Huh, Y. Choi, J.H. Jung, et al., A method to stabilize the temperature dependent performance of G-APD arrays, Nucl. Instrum. Methods Phys. Res. A 772 (2015) 83–88.

[16] J.P. He, X.B. Tang, P. Gong, et al., Rapid radionuclide identification algorithm based on the discrete cosine transform and BP neural network, Ann. Nucl. Energy 112 (2018) 1–8.

[17] Hamamatsu, MPPC (Multi-Pixel Photon Counter) S13360 series. Available at http://www.hamamatsu.com. (Accessed on December 1st, 2017).

[18] M. Georgiou, G. Borghi, S.V. Spirou, et al., First performance tests of a digital photon counter (DPC) array coupled to a CsI (Tl) crystal matrix for potential use in SPECT, Phys. Med. Biol. 59 (2014) 2415.

[19] Maxim Integrated, Programmable resolution 1-wire digital thermometer. Available at https://datasheets.maximintegrated.com. (Accessed on December 1st, 2017).

[20] P. Wang, X.B. Tang, P. Gong, et al., Design of a portable dose rate detector based on a double Geiger–Mueller counter, Nucl. Instrum. Methods Phys. Res. A 879 (2018) 147–152.

[21] M. Ramilli, Characterization of SiPM: temperature dependencies, in: IEEE Nuclear Science Symposium Conference Record, NSS'08, 2008, pp. 2467–2470.